THE JOURNAL OF PHYSICAL CHEMISTRY A

pubs.acs.org/JPCA Article

Far-Infrared Synchrotron Spectroscopy of a Potentially Important Interstellar Isotopologue of Vinyl Alcohol: CH_2CHOD

Published as part of The Journal of Physical Chemistry virtual special issue "International Symposium on Molecular Spectroscopy".

Hayley Bunn, Killian Hull, Isaac Miller, and Paul L. Raston*

Cite This: *J. Phys. Chem. A* 2020, 124, 704–710 Read Online

ACCESS | Metrics & More | Article Recommendations | Supporting Information

ABSTRACT: The far-infrared spectrum (100–500 cm^{-1}) of a d_1 isotopologue of the astrophysically important molecule, vinyl alcohol, is reported. We observed several low energy (OD) torsional bands: the fundamental and first two hot bands of the *syn* rotamer and the fundamental and first hot band of the (higher energy) *anti* rotamer. While the bands corresponding to the *anti* rotamer are somewhat obscured by rotational lines of water (making a full spectroscopic analysis unfeasible at this stage), the *syn*-vinyl alcohol bands are not, and a global fit was performed that included 4404 distinct infrared lines assigned in this work, in addition to 59 previously reported microwave lines. This simultaneous analysis of the torsional fundamental, torsional hot band, and pure rotational band of *syn*-vinyl alcohol allowed for determination of spectroscopic parameters in the first two torsionally excited states and for refinement of them in the ground state. These parameters should be useful in searches for both cold and warm CH_2CHOD in interstellar molecular clouds.

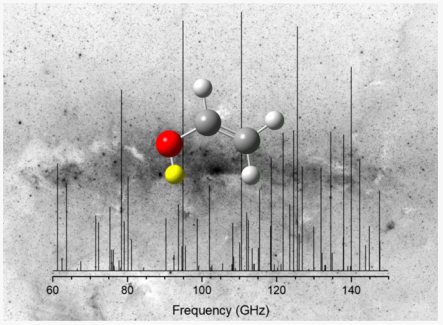

1. INTRODUCTION

An important route to the deuterium enrichment of complex organic molecules (i.e., molecules with ≥6 atoms[1]) in the interstellar medium (ISM) involves reaction with atomic deuterium on the surface of dust grains.[2] These deuterium-enriched complex molecules can then be desorbed from the grain surface into the gas phase immediately after reaction or following an ensuing increase in temperature, during, e.g., protostar formation.[2−5] One of the simplest complex organic molecules is vinyl alcohol, the normal isotopologue of which has been identified in the ISM toward Sagittarius (Sgr) B2(N).[6] It has been shown that this species is efficiently formed in proton-irradiated laboratory ices,[7] from which it can be ejected into the gas phase. One can speculate that prior to ejection, it can undergo an exchange reaction with atomic deuterium on the grain surface to produce monodeuterated vinyl alcohol (CH_2CHOD; VA-d_1).

The abundance of atomic deuterium on grain surfaces naturally depends on its abundance in the gas phase, which can be traced back to reactions involving H_2D^+.[8] It is believed that H_2D^+ is most commonly formed from the reaction between HD and H_3^+, where the abundance of H_3^+ is enhanced in regions of depleted CO, its main destroyer, which typically occurs at low temperatures as CO solidifies onto the surface of dust grains. Additionally, the reaction between HD and H_3^+ is exothermic; hence, it occurs optimally in low-temperature regions of interstellar space (T < 25 K).[9] As the temperature in the ISM increases, the rate constant for the exothermic production of H_2D^+ decreases, and eventually the reverse (endothermic) reaction is favored.[10−13] The depletion of H_2D^+ consequently impedes the deuterium enrichment of these complex molecules in warmer regions. Alternatively, it has been shown that deuterium enrichment is possible in the presence of hydrocarbons such as CH_2D^+ and C_2HD^+, which form at higher temperatures (up to 70 K).[13] Considering the complexity of the chemistry that occurs in molecular clouds, it is not surprising that there is some discrepancy between the theoretical and observed abundances of deuterated species in hot core/compact ridge regions of, for example, Orion. This could be due, in part, to not considering the deuteration of species from H_2D^+ reactions at low temperatures in existing models, occurring before the heating of the hot core.[13] All in all, detection of complex deuterated species in hot core regions allows us to comprehend the likely chemical composition of molecular clouds and how these regions have evolved.

While emission from both rotamers of the normal isotopologue of vinyl alcohol were observed toward Sgr B2(N),[6] there have not been any sightings of isotopically

Received: December 12, 2019
Revised: January 10, 2020
Published: January 10, 2020

https://dx.doi.org/10.1021/acs.jpca.9b11514
J. Phys. Chem. A 2020, 124, 704–710

labeled vinyl alcohol, the most abundant of which are expected to be the mono-^{13}C substituted vinyl alcohols and the monodeuterated vinyl alcohols (esp., CH_2CHOD).[14−16] During a microwave study reported in 1976 on *syn*-vinyl alcohol (the most stable of the two rotamers), Saito observed VA-d_1 and reported ground state (GS) rotational constants (*A*, *B*, and *C*).[17] In 1984, Rodler and Bauder also reported the microwave spectra of *syn*-vinyl alcohol along with nine minor isotopologues, including CH_2CHOD, and provided refined rotational constants (as well as higher order centrifugal distortion constants; up to the quartic level).[18] Following this, Rodler reported the microwave spectrum of the higher energy rotamer (*anti*-vinyl alcohol) and its OD equivalent and determined rotational and centrifugal distortion constants (up to the quartic level).[19] Finally, the spectroscopic coverage of isotopically substituted *syn*-vinyl alcohol was extended into the infrared (IR) region using matrix isolation techniques, where the authors assigned all but the CH stretching vibrational bands.[20]

As mentioned above, while *normal* vinyl alcohol has been observed in the ISM, minor isotopologues of vinyl alcohol have not, even though previously reported spectroscopic constants should be sufficient to allow for accurate predictions of cold transitions. On the other hand, methanol and the monodeuterated form, CH_3OD, have been extensively observed (particularly toward Orion).[21] In 1979, Gottlieb et al. reported that they observed CH_3OD toward Sgr B2;[22] however, it was not detected in a later, sensitive survey of Sgr B2 (reported in 1986).[23] In 1988, Mauersberger et al. reported observing CH_3OD in Orion-KL, reporting 13 transitions between 80 and 160 GHz.[24] In that study, they also suggested the presence of a potentially less abundant monodeuterated form, CH_2DOH. The group attempted to detect this species but due to the lack of spectroscopic data were unsuccessful. In 1993, the group reported successfully detecting this species toward Orion-KL with assistance of further unpublished spectroscopic data.[25] It has since been observed toward Sgr B2(N), along with a possible detection of CH_3OD.[2] Recently, there have also been detections of doubly deuterated[26] and triply deuterated[27] methanol.

We previously reported the far-IR gas phase spectra of both *syn*- and *anti*-vinyl alcohol and used the measured band positions to empirically refine an *ab initio* torsional potential.[28] Following this, we reported the high resolution analysis of the *anti*-vinyl alcohol OH torsional fundamental (ν_{15}),[29] thus providing spectroscopic constants useful for searches of vibrationally warm vinyl alcohol for the first time. We now expand on this by analyzing the spectrum of VA-d_1 in the far-IR, which contains both *syn*- and *anti*-vinyl alcohol torsional fundamental bands (as well as some of their hot bands); we determine band centers for both rotamers and perform a high resolution spectroscopic analysis of the *syn* rotamer that results in refinement of the ground state constants and the determination of two sets of excited state constants.

2. EXPERIMENTAL SECTION

2.1. Spectroscopy. The high resolution spectrum of CH_2CHOD was recorded using the THz/Far-IR Beamline at the Australian Synchrotron, as recently outlined.[28] Briefly, VA-d_1 was produced by pyrolyzing monodeuterated 2-chloroethanol at 950 °C. The products were continuously flowed through a room temperature multipass cell with 16 passes, providing a total path length of 10 m. The optical elements used here are the same as that used previously,[30] which included a Mylar beam splitter and polyethylene windows, in addition to a liquid helium-cooled silicon bolometer detector. The monodeuterated 2-chloroethanol was prepared by hydrogen exchange (25 mL of 2-chloroethanol with 3 × 10 mL of D_2O), followed by extraction with an equivalent amount dichloromethane (×2) and a final drying over $MgSO_4$.[31] Spectra were recorded under low- or high-flow rate conditions.

2.2. Anharmonic Frequency Calculations. For the electronic structure calculations performed in this work we utilized the Gaussian 09 package,[32] as previously described in ref 28. Anharmonic frequency calculations of monodeuterated *syn*- and *anti*-vinyl alcohol were performed, based on the coupled cluster optimized structure we previously reported,[28] which incorporated single, double, and perturbative triple excitation contributions [CCSD(T)]. Performing anharmonic corrections at lower levels of theory than a structure was optimized at has been shown to provide very accurate frequencies,[33−35] and following this we used a lower level second-order Møller−Plesset (MP2) theory for calculating anharmonic corrections. For ease of comparison, the reported harmonic frequencies are extracted from the MP2 "anharmonic" calculations. We utilized Dunning's correlation consistent quadruple ζ basis set (cc-pVQZ) throughout.[36]

2.3. Internal Rotation Hamiltonian. We previously reported an empirically refined torsional potential for vinyl alcohol that is utilized here.[28] The potential has the functional form

$$V(\phi) = \frac{1}{2}\sum_{n=1}^{7} V_n(1 - \cos n\phi) \quad (1)$$

where ϕ is the C═C−O−H dihedral angle (see inset in Figure 3). Pitzer torsional inertias for the monodeuterated isotopologue were calculated in 5° increments as previously outlined,[37] and the values were fit to the Fourier expansion

$$F(\phi) = \sum_{n=0}^{7} F_n \cos n\phi \quad (2)$$

The F_n values determined here are provided along with the previously determined V_n values[28] in Table 1. The potential energy and inertial functions are used in the internal rotation Hamiltonian

$$H = -\frac{d}{d\phi}F(\phi)\frac{d}{d\phi} + V(\phi) \quad (3)$$

Table 1. Potential Energy and Internal Rotation Fourier Series Coefficients (in cm^{-1})

potential energy parameters[a]		internal rotation parameters	
	empirically refined	F_0	13.405
V_1	168.4	F_1	0.984
V_2	1471.8	F_2	0.321
V_3	246.9	F_3	−0.0161
V_4	−35.155[b]	F_4	−0.00400
V_5	−0.371[b]	F_5	−0.00386
V_6	−2.072[b]	F_6	0.00175
V_7	0.431[b]	F_7	0.00105

[a]From ref 28. [b]Constrained to *ab initio* values.

https://dx.doi.org/10.1021/acs.jpca.9b11514
J. Phys. Chem. A 2020, 124, 704−710

to determine the torsional eigenvalues, by solving the associated Schrödinger equation. This was performed using the method of Laane and co-workers,[38,39] using an existing script.[40]

3. RESULTS AND DISCUSSION

3.1. Band Assignment and Torsional Analysis. The successful production of monodeuterated 2-chloroethanol is evident from the shift in the ν_{20} torsional band of the most stable rotamer of 2-chloroethanol (Gg′);[41,42] this shift is from 344.2 to 240.6 cm^{-1}, which is consistent with the relation, $\overline{\nu}_D \approx \overline{\nu}_H \times \sqrt{m_H/m_D} = 243\ cm^{-1}$. As shown in Figure 1, we

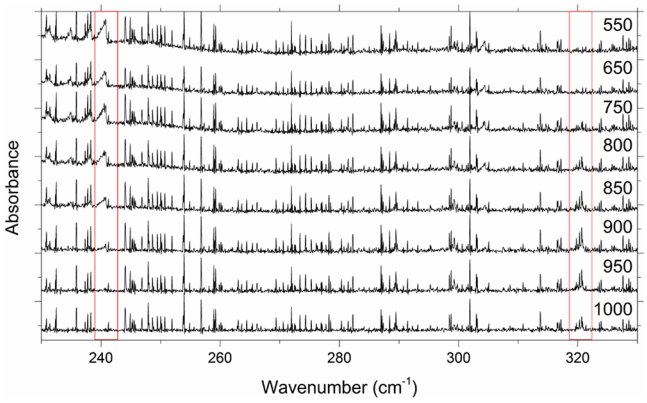

Figure 1. Low resolution (0.1 cm^{-1}) far-IR spectra showing the decrease in the monodeuterated precursor around 240 cm^{-1} and concomitant increase in VA-d_1 around 320 cm^{-1}, with increasing pyrolysis temperature (indicated for each trace; in °C).

observed a marked gradual decrease in the deuterated 2-chloroethanol precursor peak as we increased the pyrolysis temperature from 800 to 950 °C. Along with the reduction of the precursor signal we saw an increase in a feature around 320 cm^{-1}, which we assign to the *a″ c*-type OD torsional mode (ν_{15}) of *syn*-VA-d_1. This is much higher than what is expected from the above relation ($\overline{\nu}_D \approx 288\ cm^{-1}$), which suggests that the potential is somewhat less "harmonic" in the *syn* well. We note very good agreement, however, with the calculated anharmonic MP2 vibrational frequency (325 cm^{-1}).

The high resolution (0.00096 cm^{-1}) spectrum of *syn*-VA-d_1 is presented in Figure 2. Here, we see the band origin of the ν_{15} fundamental which is characterized by a strong central Q branch peak (at 320.6 cm^{-1}), in addition to its first and second torsional hot bands (centered around 299.2 and 276.3 cm^{-1}, respectively). The ν_{15} fundamental of *anti*-vinyl alcohol can also be seen in Figure 2 located around 200 cm^{-1}, with its first hot band near 196 cm^{-1}. Based on comparison to anharmonic frequency calculations (Table 2), the bands of *syn*- and *anti*-vinyl alcohol, along with their first hot bands, were easily assigned (assignment of the second hot band for the *syn* rotamer relied on the potential function; *vide infra*). Good agreement is evident for both rotamers; however, for *anti*-vinyl alcohol, the fundamental and hot band predictions are flipped relative to what is observed. We do not consider this to be very significant, however, since the residuals are all small (less than 10 cm^{-1}).

Figure 3 shows the empirically refined torsional potential of vinyl alcohol,[28] along with the eigenvalues for CH_2CHOD, determined as described above. Table 2 reports the corresponding energy level differences, showing better agreement compared to anharmonic frequency calculations with the observed band origins. As expected, the heavier deuterium atom in VA-d_1 results in a much closer spacing of the energy levels in comparison to the normal isotopologue. Naturally, this results in a higher relative population of the excited vibrational states in VA-d_1 in comparison to *normal* vinyl alcohol; however, we still observe only the first hot band (ν = 2-1) for *anti* and the first two for *syn* (ν = 2-1 and ν = 3-2). This is likely due to the reduced S/N resulting from incomplete deuteration (The ratio, VA:VA-d_1, ended up being ~1:1.2.), in addition to water contamination in the spectra. Unfortunately, the *anti*-vinyl alcohol spectral region is the most contaminated, making it difficult to perform a detailed analysis. The *syn*-vinyl alcohol region, on the other hand, is much less contaminated, allowing for a high-resolution analysis to be performed.

3.2. High-Resolution Spectroscopic Analysis. We fit the far-IR spectrum of *syn*-VA-d_1 to a Watson's *A*-reduced

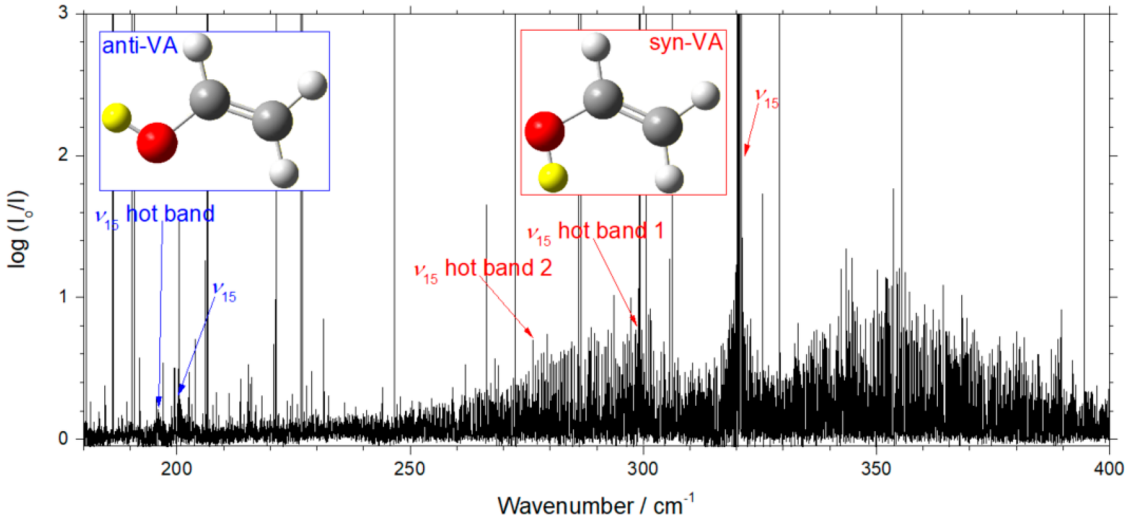

Figure 2. Survey spectrum of VA-d_1 at a relatively high flow rate. For clarity, water and HCl/DCl lines have been artificially reduced in intensity. Bands corresponding to the torsional vibration of *anti*- and *syn*-VA-d_1 are arrowed. This is a high flow-rate spectrum.

https://dx.doi.org/10.1021/acs.jpca.9b11514
J. Phys. Chem. A 2020, 124, 704−710

Table 2. Observed ν_{15} Frequencies (cm^{-1}) of Monodeuterated *syn*- and *anti*-Vinyl Alcohol in the Far-IR, in Comparison to Theoretical Ones

rotamer	ν'-ν''	observed	*ab initio* $V(\phi)$[a]	empirically refined $V(\phi)$[a]	anharmonic[b]	harmonic[b]
syn	1-0	320.6	314.7	317.4	325.3	344.9
	2-1	299.2	296.0	297.9	305.8	344.9
	3-2	276.3	275.0	275.8		344.9
anti	1-0	200.6	193.9	195.2	192.5	194.8
	2-1	196.3	193.1	195.8	193.4	194.8
	3-2		188.0	192.0		194.8

[a]Difference frequencies determined from calculated eigenstates on the appropriate double-well potential. [b]Calculated at the MP2/VQZ level.

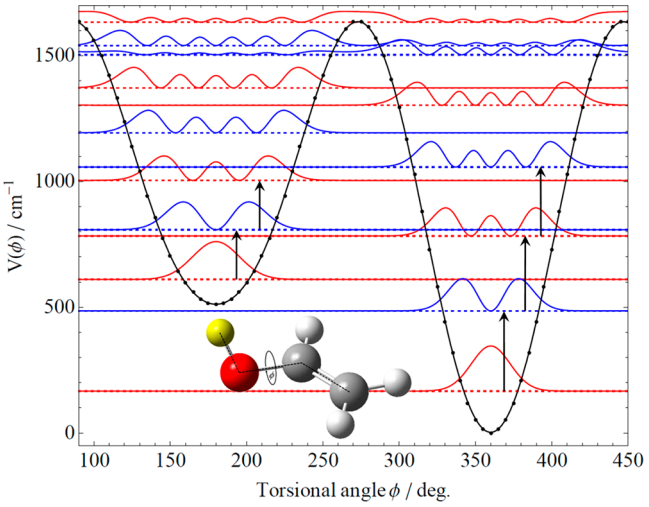

Figure 3. OH torsional potential calculated in 5° increments (black dots) fitted to a Fourier expansion (black curve); see ref 28 for details. Black arrows indicate the observed torsional bands.

Hamiltonian in the I^r representation as outlined in the following. Initially, the spectrum in the OD torsional fundamental was simulated (in PGOPHER[43]) using the GS rotational and centrifugal distortion constants from Rodler's 1984 microwave study[18] and predicted first excited state (ν_{15} = 1) constants calculated here. Isolated groups of lines within low K_a sub-bands that showed similar patterns between the experimental and simulated spectra were initially assigned, later moving into higher K_a sub-bands. Initially, only the excited state rotational constants (A, B, and C) and band origin were allowed to float, with the quartic distortion constants (Δ_K, Δ_{JK}, Δ_J, δ_K, δ_J) fixed to their GS values. After substantially improving the fit, which included systematically removing assignments with large residual errors, the quartic distortion constants were floated, starting with the largest and gradually moving on to the smallest. We found that refinement of GS constants from their initial microwave values was eventually necessary, which was assisted by inclusion of the previously reported microwave transitions, with appropriate weightings.[17,18] Inclusion of the first two sextic terms Φ_K and Φ_{KJ}, in both ground and excited states, considerably improved the fit (as monitored by the average residual error). Inclusion of Φ_{JK} and Φ_J showed minimal improvement and were set to zero.

Following this, we included the first torsional hot band in the fit, for which assignments could be made after extrapolating the parameter shifts from ν_{15} = 1 to ν_{15} = 2. Somewhat surprisingly, perturbations were absent in the hot band spectra, which made for a relatively straightforward analysis. The lack of perturbations, however, can be understood by examining Figure S1, which shows that the first and second excited torsional states are relatively well isolated from other vibrations. After refining all 32 parameters in PGOPHER, we finalized the global fit (GS, ν_{15}, and $2\nu_{15}$) using SPFIT,[44] and then PIFORM was used for data interpretation.[45] Abridged

Table 3. Observed and Calculated Vibrational, Rotational, and Higher Order Centrifugal Distortion Constants for *syn*-VA-d_1[e]

parameter	calcd[a] (GS)	exp. MW[b] (GS)	exp. MW+IR (GS)	exp. MW+IR (ν_{15})	exp. MW+IR ($2\nu_{15}$)
ν_0 (cm^{-1})				320.618225(13)[c]	619.833121(22)[c]
A (MHz)	52554	52585.52(2)	52585.5255(85)	52424.462(13)	52281.359(27)
B (MHz)	10266	10320.499(3)	10320.5006(15)	10265.2416(24)	10216.6144(37)
C (MHz)	8581	8621.184(3)	8621.1868(14)	8628.7188(21)	8635.8741(31)
Δ_J (kHz)	7.646	7.80(3)	7.7900(12)	7.6048(13)	7.5368(16)
Δ_{JK} (kHz)	−48.43	−49.2(5)	−49.496(18)	−44.488(20)	−42.641(43)
Δ_K (kHz)	599.8	607(1)	607.87(11)	599.65(10)	594.86(24)
Δ_J (kHz)	1.735	1.785(3)	1.78321(20)	1.67816(46)	1.62843(82)
Δ_K (kHz)	26.11	27.88(4)	27.823(26)	18.078(52)	14.101(94)
Φ_{KJ} (Hz)	0.3766		−3.42(11)	−4.10(10)	−4.20(27)
Φ_K (Hz)	−5.201		23.02(29)	23.06(23)	23.38(58)
N_{lines}[d]			4404 IR + 59 MW		
max. J, K_a			62, 22		
σ_{rms} MW (kHz)			68.19		
σ_{rms} IR (MHz)			4.48		

[a]Calculated at the MP2/VQZ level on a CCSD(T)/VQZ optimized structure. [b]From ref 18. [c]Uncertainty in the band origin does not include calibration error; we expect this is less than 0.0001 cm^{-1} after calibration using residual water lines.[51] [d]Number of distinct lines; blended lines were given a weighting of $1/n$ (n is the number of lines in the blend). [e]Uncertainty (1σ error) in the last digit is indicated in parentheses.

https://dx.doi.org/10.1021/acs.jpca.9b11514
J. Phys. Chem. A 2020, 124, 704−710

output files are available in the Supporting Information. A total of 4404 unique IR lines have been assigned and included in the fit with a maximum J' of 62 and K_a' of 22. A total of 59 microwave transitions were also included from previous reports,[17,18] with a maximum J' of 22 and K_a' of 5; they were given a weighting of 72 or 360 times that of the IR transitions, depending on the estimated accuracy in the microwave studies (20 or 100 kHz). Table 3 summarizes the resulting parameters from the spectroscopic analysis of *syn*-VA-d_1.

We see good agreement between the experimental constants with those derived from anharmonic frequency calculations, indicating physically meaningful values. There is, however, a discrepancy in the sextic terms, Φ_K and Φ_{KJ}, where we observed similar values with opposite signs. It has been previously noted that sextic constants are largely affected by the reduction of the Hamiltonian,[46] commonly leading to slight discrepancies and inconsistencies with the sign, when compared with experimental values. The quality of the final fundamental and hot band fit is apparent in Figures 4 and 5,

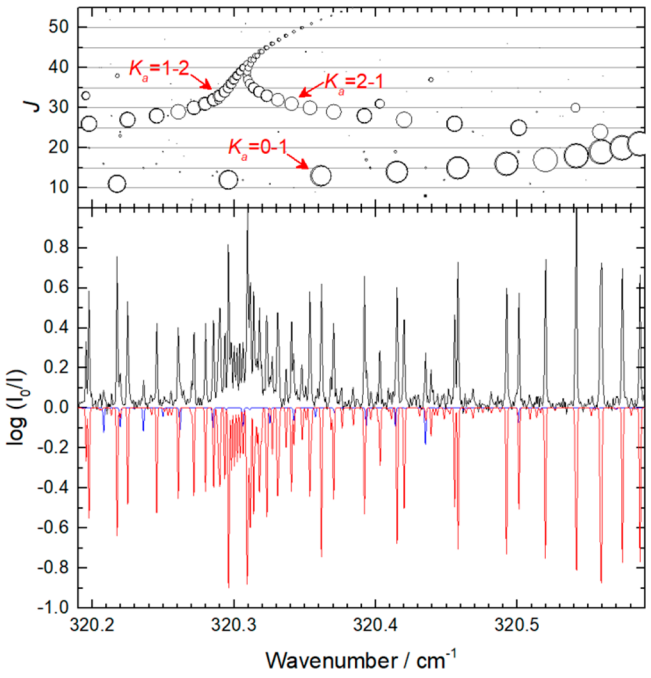

Figure 4. Close-up of the second most intense Q branch in the fundamental band of *syn*-VA-d_1. The experimental spectrum (black) is shown along with the simulated fundamental band (red) and hot band (blue). The upper panel shows the associated Fortrat diagram. This is a low flow-rate spectrum.

respectively, which shows the second most intense Q-branch within each of the torsional bands. We wish to note that due to the low intensity of the second hot band in addition to its interference by water lines, this band was not included in the fit. Future efforts will focus on obtaining a clean high-resolution spectrum, free of water, for VA-d_1. This will further improve the current *syn*-vinyl alcohol fit and allow for a high-resolution analysis of the *anti* rotamer to be performed.

3.3. Astrophysical Relevance. It is interesting to speculate on the possibility of detecting emission from CH_2CHOD in the ISM. We can make some qualitative estimations, drawing from available observational data on CH_3OH, CH_3OD, and CH_2CHOH. The column density of

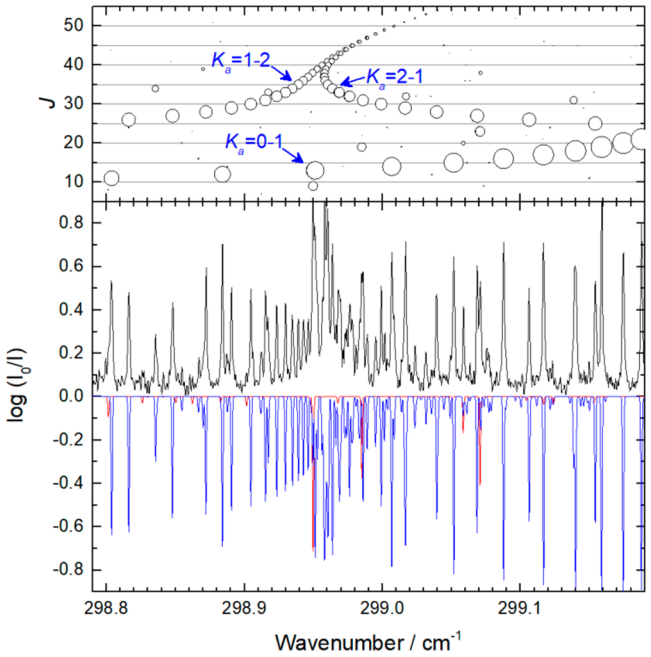

Figure 5. Same as Figure 4 but in the vicinity of the first hot band. This is a high flow-rate spectrum.

syn- and *anti*-vinyl alcohol was reported from the millimeter wave detection of vinyl alcohol toward Sgr B2(N), to be 2.0×10^{14} cm^{-2} and 2.4×10^{13} cm^{-2}, respectively, giving a total column density for *normal* vinyl alcohol of 2.24×10^{14} cm^{-2}.[6] The ratio of CH_3OD/CH_3OH was originally (effectively) reported as 0.007;[22] however, recent observations provide a stringent upper limit that is 1 order of magnitude lower (0.0007).[2] Assuming the deuteration ratio for vinyl alcohol (CH_2CHOD/CH_2CHOH) is the same as the (new) upper limit for methanol (0.0007), the total (*syn* + *anti*) VA-d_1 abundance will be 1.6×10^{11} cm^{-2}. Assuming the same relative abundance of the rotamers, this gives a *syn*- and *anti*-VA-d_1 column density of 1.4×10^{11} cm^{-2} and 1.7×10^{10} cm^{-2}, respectively. These values are considerably lower than the detected column densities of most interstellar molecules, e.g., in a survey of deuterated complex organic molecules in Sgr B2(N) using the Atacama Large Millimeter/submillimeter Array (ALMA), the lowest observed column density was 3×10^{14} cm^{-2}.[2]

There are, however, reported detections of molecules (with larger dipole moments) that have lower column densities than this (3×10^{14} cm^{-2}). For example, Bacmann et al. reported the identification of D_2CO at a column density of 5.8×10^{11} cm^{-2}, using the IRAM 30 m telescope.[47] D_2CO has a dipole moment (a axis only) of 2.347122 D[48] which is larger than that for vinyl alcohol, with a and b axis dipole moments of 0.616 and 0.807 D for the *syn* rotamer and 0.547 and 1.702 D for the *anti* rotamer. As the intensity of a transition is proportional to the square of the dipole moment, the probability of observing VA-d_1 in the ISM is comparatively (but not vanishingly) low. The best-case scenario, considering only the column densities and dipole moment squares, shows that an a-type (b-type) emission of *syn*-VA-d_1 is 19 (35) times less likely to be observed than formaldehyde [65 (628) for b-type (a-type) of *anti*-VA-d_1]. It should be noted that in addition to this, the partition function of vinyl alcohol is less favorable, resulting from the three additional atoms (in comparison to form-

https://dx.doi.org/10.1021/acs.jpca.9b11514
J. Phys. Chem. A 2020, 124, 704−710

aldehyde). Nonetheless, if successful, the detection (and determination of relative abundance) of VA-d_1 would allow for a better understanding of how vinyl alcohol forms in the ISM. It is hoped that our refined ground state constants, in particular, might eventually be useful in performing efficient searches for this species.

4. SUMMARY AND OUTLOOK

Here we reported the far-IR spectrum and analysis of monodeuterated vinyl alcohol (CH_2CHOD; VA-d_1). We observed the ν_{15} OD torsional fundamental and its first two hot bands for *syn*-vinyl alcohol (at 320.6, 299.2, and 276.3 cm^{-1} respectively), along with the fundamental and first hot band of *anti*-vinyl alcohol (at 200.6 and 196.3 cm^{-1}). The band centers agree very well with the previously reported semi-experimental potential energy surface, with a RMS deviation between experimental and theoretical torsional energies of 2.9 cm^{-1}. A high resolution analysis of the *syn*-vinyl alcohol fundamental and first hot band has been performed, resulting in vibrational, rotational, and centrifugal distortion constants (including quartic and the first two sextic terms) for ν_{15} = 0, 1, and 2. The analysis reported here could be of assistance in searches for VA-d_1 in warm environments, since our ground state and excited state rotational constants should allow for accurate predictions to be made up to several hundred Kelvin. In closing, we note that recent searches for the normal isotopologue of vinyl alcohol have been made, and while they have been unsuccessful,[49,50] neither attempted to observe this somewhat elusive species toward the source where it was originally observed.[6]

ASSOCIATED CONTENT

Supporting Information

The Supporting Information is available free of charge at https://pubs.acs.org/doi/10.1021/acs.jpca.9b11514.

Energy level diagram for *syn*-VA-d_1 (Figure S1); close-up in the K_a = 4−5 sub-band of *syn*-VA-d_1 (Figure S2); and simulated pure rotational spectrum of *syn*-VA-d_1 at 10 K (Figure S3) (PDF)

Abridged output file from the fit (TXT)

Observed transitions, assignments, residuals, and weights (for blended lines) for *syn*-VA-d_1 (Table S1) (TXT)

AUTHOR INFORMATION

Corresponding Author

Paul L. Raston − *University of Adelaide, Adelaide, Australia, and James Madison University, Harrisonburg, Virginia;* orcid.org/0000-0003-3717-4154; Email: rastonpl@jmu.edu

Other Authors

Hayley Bunn − *University of Adelaide, Adelaide, Australia*

Killian Hull − *James Madison University, Harrisonburg, Virginia*

Isaac Miller − *James Madison University, Harrisonburg, Virginia*

Complete contact information is available at: https://pubs.acs.org/10.1021/acs.jpca.9b11514

Notes

The authors declare no competing financial interest.

ACKNOWLEDGMENTS

Acknowledgment is made to the National Science Foundation (NSF-REU CHE-1757874) and the Research Corporation for Science Advancement (Cottrell Scholar Award). Experiments were conducted at the High Resolution Far-IR Beamline at the Australian Synchrotron, Victoria, Australia. This research used high-performance computing services provided by eRSA. We are pleased to contribute this manuscript to the VSI celebrating the 75th anniversary of the International Symposium on Molecular Spectroscopy, which has been a continuous source of inspiration and enlightenment. We wish to thank Alexander Gentleman for providing valuable technical advice.

REFERENCES

(1) Herbst, E.; van Dishoeck, E. F. Complex Organic Interstellar Molecules. *Annu. Rev. Astron. Astrophys.* **2009**, *47*, 427−480.

(2) Belloche, A.; Müller, H. S. P.; Garrod, R. T.; Menten, K. M. Exploring Molecular Complexity with ALMA (EMoCA): Deuterated Complex Organic Molecules in Sagittarius B2(N2). *Astron. Astrophys.* **2016**, *587*, A91.

(3) Walmsley, C. M.; Hermsen, W.; Henkel, C.; Mauersberger, R.; Wilson, T. L. Deuterated Ammonia in the Orion Hot Core. *Astrophys. J.* **1987**, *172*, 311−315.

(4) Turner, B. E. Detection of doubly deuterated interstellar formaldehyde (D_2CO): an indicator of active grain surface chemistry. *Astrophys. J.* **1990**, *362*, L29−L33.

(5) Ceccarelli, C.; Caselli, P.; Bockelée-Morvan, D.; Mousis, O.; Pizzarello, S.; Robert, F.; Semenov, D., Deuterium Fractionation: The Ariadne's Thread from the Pre-collapse Phase to Meteorites and Comets today. In *Protostars and Planets VI*, University of Arizona Press: 2014; pp 859−882, DOI: 10.2458/azu_uapress_9780816531240-ch037.

(6) Turner, B. E.; Apponi, A. J. Microwave Detection of Interstellar Vinyl Alcohol CH_2=CHOH. *Astrophys. J.* **2001**, *561*, L207−L210.

(7) Hudson, R. L.; Moore, M. H. Solid-Phase Formation of Interstellar Vinyl Alcohol. *Astrophys. J.* **2003**, *586*, L107−L110.

(8) Tielens, A. G. G. M. Surface Chemistry of Deuterated Molecules. *Astron. Astrophys.* **1983**, *119*, 177−184.

(9) Tielens, A. G. G. M. *The Physics and Chemistry of the Interstellar Medium*; Cambridge University Press: 2005; DOI: 10.1017/CBO9780511819056.

(10) Adams, N. G.; Smith, D. A Laboratory Study of the Reaction H_3^+ + HD ≤ > H_2D^+ + H_2: The Electron Densities and the Temperatures in Interstellar Clouds. *Astrophys. J.* **1981**, *248*, 373−379.

(11) Herbst, E. The Temperature Dependence of the HCO^+/DCO^+ Abundance Ratio in Dense Interstallar Clouds. *Astron. Astrophys.* **1982**, *111*, 76−80.

(12) Smith, D.; Adams, G.; Alge, E. Some H/D Exchaange Reactions Incolved in Deuteration of Interstellar Molecules. *Astrophys. J.* **1982**, *263*, 123−129.

(13) Millar, T. J.; Bennett, A.; Herbst, E. Deuterium Fractionation in Dense Interstellar Clouds. *Astrophys. J.* **1989**, *340*, 906−920.

(14) Savage, C.; Apponi, A. J.; Ziurys, L. M.; Wyckoff, S. Galactic $^{12}C/^{13}C$ Ratios from Millimeter-Wave Observations of Interstellar CN. *Astrophys. J.* **2002**, *578* (1), 211−223.

(15) Jacq, T.; Baudry, A.; Walmsley, C.; Caselli, P. Deuterium in the Sagittarius B2 and Sagittarius A galactic center regions. *Astron. Astrophys.* **1999**, *347*, 957−966.

(16) Wilson, T. L.; Rood, R. T. Abundances in the Interstellar Medium. *Annu. Rev. Astron. Astrophys.* **1994**, *32* (1), 191−226.

(17) Saito, S. Microwave Spectroscopic Detection of Vinyl Alcohol, CH_2=CHOH. *Chem. Phys. Lett.* **1976**, *42* (3), 399−402.

(18) Rodler, M.; Bauder, A. Structure of *syn*-Vinyl Alcohol Determined by Microwave Spectroscopy. *J. Am. Chem. Soc.* **1984**, *106*, 4025−4028.

(19) Rodler, M. Micorwave Spectrum, Dipole Moment, and Structure of Anti-Vinyl Alcohol. *J. Mol. Spectrosc.* **1985**, *114*, 23−30.
(20) Rodler, M.; Blom, C. E.; Bauder, A. Infrared Spectrum and General Valence Force Field of syn-Vinyl Alcohol. *J. Am. Chem. Soc.* **1984**, *106*, 4029−4035.
(21) Ball, J. A.; Gottlieb, C. A.; Lilley, A. E.; Radford, H. E. Detection of Methyl Alcohol in Sagittarius. *Astrophys. J.* **1970**, *162*, L203.
(22) Gottlieb, C. A.; Ball, J. A.; Gottlieb, E. W.; Dickinson, D. F. Interstellar Methyl Alcohol. *Astrophys. J.* **1979**, *227*, 422−432.
(23) Cummins, S. E.; Linke, R. A.; Thaddeus, P. A Survey of the Millimeter-wave Spectrum of Sagittarius B2. *Astrophys. J., Suppl. Ser.* **1986**, *60*, 819−878.
(24) Mauersberger, R.; Henkel, C.; Jacq, T.; Walmsley, C. M. Deuterated Methanol in Orion. *Astron. Astrophys.* **1988**, *194*, L1−L4.
(25) Jacq, T.; Walmsley, C. M.; Mauersberger, R.; Anderson, T.; Herbst, E.; De Lucia, F. C. Detection of Interstellar CH_2DOH. *Astron. Astrophys.* **1993**, *271*, 276−281.
(26) Parise, B.; Ceccarelli, C.; Tielens, A. G. G. M.; Herbst, E.; Lefloch, B.; Caux, E.; Castets, A.; Mukhopadhyay, I.; Pagani, L.; Loinard, L. Detection of Doubly-deuterated Methanol in the Solar-type Protostar IRAS 16293−2422. *Astron. Astrophys.* **2002**, *393* (3), L49−L53.
(27) Parise, B.; Castets, A.; Herbst, E.; Caux, E.; Ceccarelli, C.; Mukhopadhyay, I.; Tielens, A. G. G. M. J. A. First Detection of Triply-deuterated Methanol. *Astron. Astrophys.* **2004**, *416* (1), 159−163.
(28) Bunn, H.; Hudson, R. J.; Gentleman, A. S.; Raston, P. L. Far-Infrared Synchrotron Spectroscopy and Torsional Analysis of the Important Interstellar Molecule, Vinyl Alcohol. *ACS Earth and Space Chemistry* **2017**, *1* (2), 70−79.
(29) Bunn, H.; Soliday, R. M.; Sumner, I.; Raston, P. L. Far-infrared Spectroscopic Characterization of Anti-vinyl Alcohol. *Astrophys. J.* **2017**, *847* (1), 67.
(30) Bunn, H.; Bennett, T.; Karaylian, A.; Raston, P. L. Far-Infrared Spectroscopy of the H_2-O_2 van der Waals Complex. *Astrophys. J.* **2015**, *799*, 65.
(31) We note that MgO would have been a more appropriate drying agent, which could have avoided spectral contamination by water lines.
(32) Frisch, M. J.; Trucks, G. W.; Schlegel, H. B.; Scuseria, G. E.; Robb, M. A.; Cheeseman, J. R.; Scalmani, G.; Barone, V.; Mennucci, B.; Petersson, G. A., et al. *Gaussian 09*; Gaussian, Inc.: Wallingford, CT, USA, 2009.
(33) Barone, V. Anharmonic Vibrational Properties by a Fully Automated Second-order Perturbative Approach. *J. Chem. Phys.* **2005**, *122* (1), 014108.
(34) Rauhut, G.; Barone, V.; Schwerdtfeger, P. Vibrational Analyses for CHFClBr and CDFClBr Based on High Level *Ab Initio* Calculations. *J. Chem. Phys.* **2006**, *125* (5), 054308.
(35) Miliordos, E.; Aprà, E.; Xantheas, S. S. Optimal Geometries and Harmonic Vibrational Frequencies of the Global Minima of Water Clusters $(H2O)_n$, n = 2−6, and Several Hexamer Local Minima at the CCSD(T) Level of Theory. *J. Chem. Phys.* **2013**, *139* (11), 114302.
(36) Dunning, T. H., Jr. Gaussian basis sets for use in correlated molecular calculations. I. The atoms boron through neon and hydrogen. *J. Chem. Phys.* **1989**, *90* (2), 1007−1023.
(37) Wong, B. M.; Thom, R. L.; Field, R. W. Accurate Inertias for Large-Amplitude Motions: Improvements on Prevailing Approximations. *J. Phys. Chem. A* **2006**, *110* (23), 7406−7413.
(38) Laane, J. One-Dimensional Potential Energy Functions in Vibrational Spectroscopy. *Q. Rev., Chem. Soc.* **1971**, *25* (4), 533−552.
(39) Lewis, J. D.; Malloy, T. B. J.; Chao, T. H.; Laane, J. Periodic Potential Functions for Pseudorotation and Internal Rotation. *J. Mol. Struct.* **1972**, *12*, 427−449.
(40) Liang, T.; Magers, D. B.; Raston, P. L.; Allen, W. D.; Douberly, G. E. Dipole Moment of the HOOO Radical: Resolution of a Structural Enigma. *J. Phys. Chem. Lett.* **2013**, *4* (21), 3584−3589.
(41) Durig, J. R.; Zhou, L.; Gounev, T. K.; Klaeboe, P.; Guirgis, G. A.; Wang, L. F. Far Infrared Spectra, Confromational Equilibria, Vibrational Assignments and *Ab Initio* Calculations of 2-Chloroethanol. *J. Mol. Struct.* **1996**, *385*, 7−21.
(42) Soliday, R. M.; Bunn, H.; Sumner, I.; Raston, P. L. Far-Infrared Synchrotron Spectroscopy and Quantum Chemical Calculations of the Potentially Important Interstellar Molecule, 2-Chloroethanol. *J. Phys. Chem. A* **2019**, *123* (6), 1208−1216.
(43) Western, C. M. PGOPHER: A Program for Simulating Rotational, Vibrational and Electronic Spectra. *J. Quant. Spectrosc. Radiat. Transfer* **2017**, *186*, 221−242.
(44) Pickett, H. M. The Fitting and Prediction of Vibration-rotation Spectra with Spin Interactions. *J. Mol. Spectrosc.* **1991**, *148* (2), 371−377.
(45) Kisiel, Z. *PIFORM*; 2017. http://www.ifpan.edu.pl/~kisiel/asym/asym.htm#piform (accessed Jan 15, 2020).
(46) D'Eu, J.-F.; Demaison, J.; Burger, H. Millimeter-wave and High-resolution FTIR Spectroscopy of SiH_2F_2: the Ground and v_4=1 States. *J. Mol. Spectrosc.* **2003**, *218*, 12−21.
(47) Bacmann, A.; Lefloch, B.; Ceccarelli, C.; Steinacker, J.; Castets, A.; Loinard, L. CO Depletion and Deuterium Fractionation in Prestellar Cores. *Astrophys. J.* **2003**, *585*, L55−L58.
(48) Fabricant, B.; Krieger, D.; Muenter, J. S. Molecular Beam Electric Resonance Study of Formaldehyde, Thioformaldehyde, and Ketene. *J. Chem. Phys.* **1977**, *67* (4), 1576−1586.
(49) Martin-Drumel, M.-A.; Lee, K. L. K.; Belloche, A.; Zingsheim, O.; Thorwirth, S.; Müller, H. S. P.; Lewen, F.; Garrod, R. T.; Menten, K. M.; McCarthy, M. C.; et al. Submillimeter Spectroscopy and Astronomical Searches of Vinyl Mercaptan. *Astron. Astrophys.* **2019**, *623*, A167.
(50) Melosso, M.; McGuire, B. A.; Tamassia, F.; Degli Esposti, C.; Dore, L. Astronomical Search of Vinyl Alcohol Assisted by Submillimeter Spectroscopy. *ACS Earth and Space Chemistry* **2019**, *3* (7), 1189−1195.
(51) Rothman, L. S.; Gordon, I. E.; Babikov, Y.; Barbe, A.; Benner, D. C.; Bernath, P. F.; Birk, M.; Bizzocchi, L.; Boudon, V.; Brown, L. R.; et al. The HITRAN 2012 molecular spectroscopic database. *J. Quant. Spectrosc. Radiat. Transfer* **2013**, *130*, 4−50.

https://dx.doi.org/10.1021/acs.jpca.9b11514
J. Phys. Chem. A 2020, 124, 704−710